Structure and morphology of segmented polyurethanes: 2. Influence of reactant incompatibility

C. H. Y. Chen, R. M. Briber, E. L. Thomas, M. Xu†, and W. J. MacKnight
Polymer Science and Engineering Department, University of Massachusetts, Amherst, Massachusetts 01003, *USA*
(*Received* 27 *September* 1982)

By following the copolymerization of a model polyurethane system, HTPBD/2,6 (or 2,4)–TDI/BDO, by optical microscopy, it was found that initial reactant incompatibility was the key factor in determining the final morphology of bulk sample. Based on this finding and the esults from the previous paper, models are proposed to describe the morphology during polymerization of this particular polyurethane system for several hard segment compositions where both macro-phase separation and micro-phase separation of reactants can occur during polymerization. The copolymerization of one seemingly compatible system, PPO–EO/MDI/BDO, which has been previously studied and commercially produced, was also followed by optical microscopy. In the size range which can be detected with an optical microscope using conventional optics, no heterogeneities were observable at the beginning of this reaction but phase separation was evident later in the reaction and can be xplained by the presence of micro-phase separation of reactants. Globule and spherulite formation and the presence of multiple T_g's and T_m's observed by previous workers can be explained by the two levels of heterogenities present during polymerization.

Keywords Polyurethane; incompatibility; phase separation; molecular segregation; morphology

INTRODUCTION

The importance of phase separation in thermoplastic polyurethane elastomers in determining structure–property relationships was first pointed out by Cooper and Tobolsky[1]. Later, Bonart[2] and Clough *et al.*[3] investigated the scale of the microdomain structure which results from phase segregation of the hard and soft segments units. Since then, the micro-heterogeneous nature of polyurethanes has been the subject of numerous investigations[4-15], and many models of phase segregated polyurethane systems[2,16-19] have been proposed. Strong physical association, such as hydrogen bonding and/or crystallization between hard segments causes the dispersed hard domains to act as pseudo crosslinks for the flexible soft phase[20]. It has always been tacitly assumed that the copolymerization starts from a homogeneous mixture of monomers and that during polymerization and subsequent solidification, the hard and soft segments of the multiblock molecules undergo microphase separation into hard and soft domains on the order of a few hundred angstroms or less. According to Peebles[21,22], the sequence length distribution of hard blocks in such segmented polyurethanes can be represented by the most probable distribution modified by the appropriate reactivity ratios.

Recently, workers have begun to examine the question of phase separation during polymerization. Castro *et al.*[23] followed the amount of light transmitted by the sample and the increase in viscosity of a reacting mixture of polyurethane monomers, and suggested that at the onset of phase separation in the system the number average hard segment sequence length was *ca.* 1.3. Subsequent work by Hager *et al.*[24] using d.s.c. and by Camargo[25] using Fourier transform infra-red spectroscopy, found similar evidence for phase separation during the reaction on the same polyurethane system. Models of phase separation during polymerization were proposed by Nesterov *et al.*[26], and Tirrell *et al.*[27] for polyurethanes and Xu *et al.*[28] for polyether–polyesters. Recently, Foks *et al.*[29] suggested that a variety of reaction products, such as homopolymers of the hard and the soft segments, statistical copolymers or polymers crosslinked through allophanate bonding, could be expected depending on temperature and the degree to which the reactants were blended. However, the present study shows that for some polyurethane systems, because of the *incompatibility of reactants*, the compolymerization occurs from an initially heterogeneous system, and the composition of the final product is controlled by the diffusion rates of species from one phase to another and the reaction rates between different functional groups.

The present work is concerned with further defining the important factor of the reactant-reactant compatibility which strongly affects product characteristics such as hard segment length distribution (which was discussed in the previous paper)[30], molecular weight distribution and final morphology of the polymerized samples. Two particular polyurethane systems were chosen for the study; one involves a two-stage polymerization and the other a single-stage polymerization. The two-stage polymerized system was a model system based on toluene diisocyanate

* Permanent Address: Institute of Chemistry, Academia Sinica, Beijing, China.

0032-3861/83/101333-08$03.00

(TDI) (both the crystallizable 2,6-TDI and the non-crystallizable 2,4-TDI isomers were used for comparison), with 1,4-butanediol (BDO) as chain extender, and with hydroxy-terminated polybutadiene (HTPBD) as the soft segment. Unlike conventional polyurethanes with polyester or polyether soft segment, all hydrogen bonds in this system are restricted to be within the hard segments. Moreover, because no catalyst was involved, reaction kinetics were slow and manageable. At the second step of the copolymerization, the reaction was followed by a video system interfaced with an optical microscope, and macro-phase separation among reactants was found on the micron scale. After polymerization bulk samples were cryo-microtomed for both electron and optical microscopy to confirm this finding. A similar HTPBD/TDI BDO system and synthesis procedure were previously used by Brunette *et al.*[31,32]. Both dynamic mechanical and differential scanning calorimetry (DSC) data indicated the presence of *two* hard segment glass transition temperatures for the 2,4-TDI based sample having intermediate hard segment content. It was suggested that this was due to two different populations of hard segment lengths. This view was experimentally confirmed in our first paper[30], and a bimodal sequence length distribution was proposed. In the present paper, further morphological and the analytical results are presented and a model is proposed in which both macro-phase separation (on the order of microns) and micro-phase separation (on the order of 100 Å) are suggested.

For the single stage polymerization study, a system based on 4.4′-diphenyl methane diisocyanate (MDI), with BDO as chain extender, and poly(propylene oxide) endcapped with poly(ethylene oxide) (PPO–EO) as soft segment was chosen. This reaction was also studied in the optical microscope. No initial macro-phase separation was found, as was seen in the HTPBD systems, but micron size structures developed during the polymerization. The model of the micro-phase separation of reactants can be applied to explain the result. This polyurethane system has been previously investigated by Zdrahala *et al.*[33] and Change *et al.*[34] and Castro *et al.*[23].

Both hard segment rich globules and spherulites have been observed and discussed separately in the literature[34–36] (ref 36 Figure 25d) with no explanation of the relationship between the two structures given. In the present study, it was found that for the HTPBD system both globules and spherulites originate from the phase-separated monomer droplets, and spherulites were, in fact, nucleated and crystallized globules. The globules observed in the PPO–EO system may be due to a similar phenomenon.

EXPERIMENTAL

Materials

HTPBD/TDI/BDO. The HTPBD (Japanese Synthetic Rubber) had a functionality of 1.97 and $M_n = 2200$, and was used as received. The 2,6-TDI (Aldrich), 2,4-TDI (Aldrich) and BDO (Du Pont) were distilled before use. Samples of both 2,6-TDI and 2-4-TDI of composition HTPBD/TDI/BDO = 1/8/7 mole ratio were made. This composition was 49% hard segment by weight.

PPO–EO/MDI/BDO. The polypropylene oxide was endcapped with 30% (by weight) polyethylene oxide (Union Carbide) and had a functionality of 1.96 and $M_n = 2000$. Both the PPO–EO and BDO were stored over molecular sieves prior to use while the MDI (Mobay) was used as received. A sample of composition PPO–EO/MDI/BDO = 1/3.2/2.2 mole ratio was made. This composition was 31% hard segment by weight. The catalyst concentration was 0.01% dibutyl tin dilaurate by total weight.

Synthesis

HTPBD/TDI/BDO. The synthesis of the bulk sample was carried out by a conventional two-step method[31]. The procedure was as follows:

Stage I: HTPBD was endcapped with excess TDI at 120°C for one hour under a nitrogen purge.

Stage II: At 80°C, after the addition of the chain extender, the reaction mixture was mechanically stirred for two and one-half minutes, degassed, and poured into a mould.

Curing was done at 120°C for 17 h. The resulting bulk samples were 2 mm thick. For the optical microscopy study aliquots were removed early in stage II of the reaction and examined in the optical microscope.

PPO–EO/MDI/BDO. The PPO–EO/MDI/BDO system was polymerized in a one-step batch reaction where all the monomers are mixed together at 80°C. An aliquot was removed early in the reaction and examined in the optical microscope. The final morphology of the bulk sample has been the subject of a previous publication[34], and was not examined in this study.

Optical microscopy

The copolymerizations were followed by a video system interfaced to a Zeiss polarizing microscope equipped with a Mettler hot stage using magnifications of 20× to 400×. The video system was composed of a black and white Hitachi TV camera and a Panasonic video cassette recorder with Setchell and Carlson black and white TV monitor. Micrographs were taken on Kodak Tri-X film using a standard 35 mm camera back coupled to the Zeiss microscope. The morphology of the bulk samples which were made by the two stage reaction were also investigated by observing the microtomed sections.

Cryo ultra-microtomy

The samples were microtomed to examine the morphology developed during polymerization. A Sorvall MT-2B Porter-Blum ultramicrotome with a cryo thin sectioning attachment and glass knife were used. All microtomy was done in the temperature range of −75° to −65°C. Both dry knife and wet knife (with the knife trough filled with propyl alcohol for floating sections) techniques were used. Thicker sections were saved for optical microscopy and thinner sections (less than 1000 Å thick) were picked up with 300 or 400 mesh copper grids for electron microscopy.

Electron microscopy

A JEOL 100CX transmission electron microscope (TEM) was operated at 100 KV at magnifications of 2 000 × to 50 000 × using Kodak S0163 plates. Both microtomed sections and solution cast films were observed directly without support film. Special precautions were taken to minimize electron beam damage of the samples and avoid radiation artifacts by focusing on an area and

translating to an adjacent area for recording. TEM observations are reported only on the HTPBD/TDI/BDO system.

RESULTS AND DISCUSSION

HTPBD/2,6–TDI/BDO

Optical microscopy. During the initial endcapping reaction (Stage I), the reacting fluid, large excess amount of TDI along with the TDI end-capped HTPBD (designated PBD), was transparent and appeared homogeneous in the optical microscope. When BDO was added, because of the high degree of incompatibility between BDO and endcapped polybutadiene (PBD), the BDO formed a separate phase and was broken into small droplets due to the mechanical stirring. After 30 seconds of rapid stirring, a small portion of the reacting mixture was taken and pressed into a thin film of about 0.2 mm thickness between two thin glass slides. The specimen was kept at the reaction temperature (80°C), and the reaction in a fixed area was followed by optical microscopy using partially cross-polarized light, i.e., the angle between polarizer and analyzer was about 70°. *Figure 1a* shows the morphology of the specimen at 1 min after the addition of BDO. The dispersed spherical particles are BDO droplets, the size of which depends on the design and speed of the stirring device. BDO droplets were quite mobile at this point within the continuous PBD–TDI phase due to flow induced by the weight of the top cover glass and the reaction heat released. Occasionally, the BDO droplets coalesce and form irregular shapes as indicated by arrows A in *Figure 1b* and *Figure 1c*. As the reaction proceeds the TDI diffuses into the BDO droplets. The PBD diffuses only slowly into the BDO droplets due to its large size and its incompatibility with BDO and reacts mostly at the boundary of the droplets. Consequently, the BDO droplets react almost entirely with TDI to become regions of virtually pure hard segment polymer. The PBD and TDI in the continuous phase also react with each other to form an essentially pure soft segment polymer matrix. Some BDO will diffuse out of the droplets and react to form short sequences of hard segment in the matrix. The final polymer turns out to be far from a random block copolymer.

Serial micrographs taken at 30 s intervals show how the hard segment crystallinity developed during the reaction (see *Figures 1b–1e*). At approximately 3 min after the BDO was added, the system became stationary due to high viscosity. *Figure 1e* shows that at this point, not all hard phase regions appear birefringent (see arrows G in *Figures 1d* and *1e*). Because both types of hard segment regions originated from the BDO droplets, there should not be any significant difference of final hard segment content within the two kinds of regions. A reasonable explanation for the structural differences is that within some original BDO droplets, nuclei were present such as dirt particles, initiating crystallization of the polymerizing hard segment. Those original BDO droplets which did not contain any nuclei never crystallized but became the amorphous hard-segment structures termed globules in the literature[34,35]. To support this explanation of the origin of spherulite *versus* globule formation, crystals of 2,6-TDI dimer and trimer were added to the pure BDO to serve as nucleation seeds, and then this BDO was used in the second step of the reaction. The result was that almost all the polymerizing BDO droplets became crystalline before the system became stationary which indicated that the presence of a heterogeneous nucleus determined the final droplet structure.

For the bulk sample prepared by the conventional method, the mixing was at higher speeds and for longer time. Hence, in the bulk sample the hard segment regions should have a smaller average size than in the thin film sample. This was observed by both optical and electron microscopy of the microtomed bulk sample (see next section). Similar spherical phases were observed in the bulk as in the thin film sample, but fewer features could be

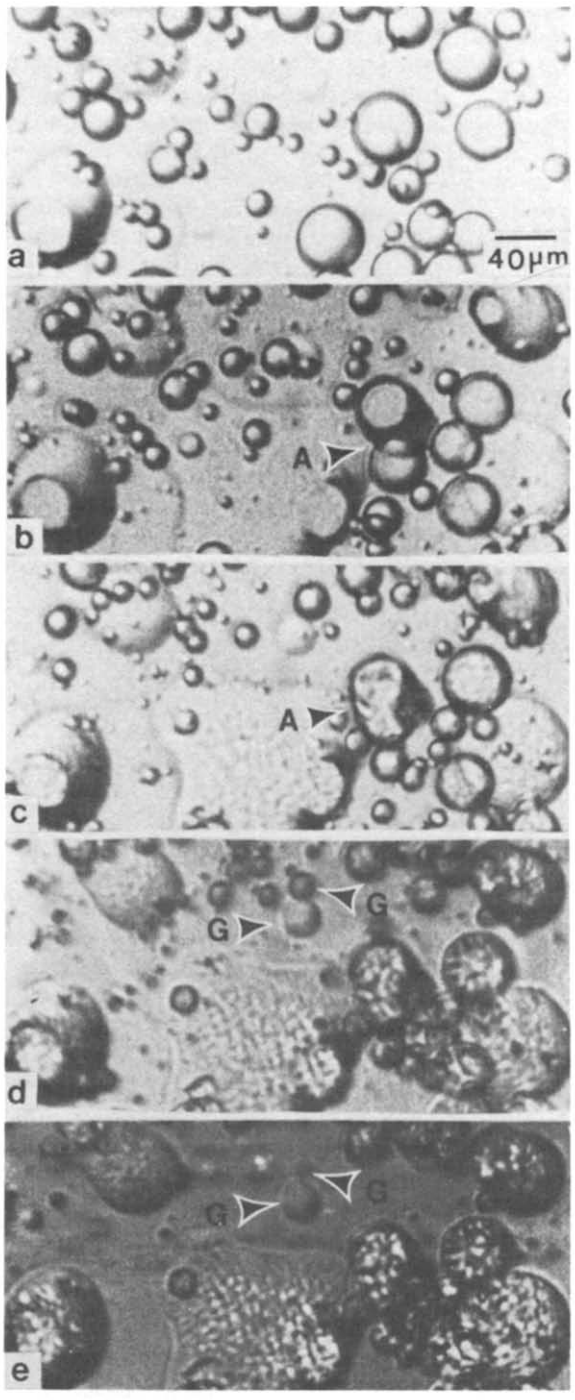

Figure 1 Optical micrographs (partially crossed polarizers) of the reacting HTPBD/2,6–TDI/BDO system. All micrographs are at the same magnification. (a) 1 min after the mixing of the second step of the reaction. (b) 1.5 min. (c) 2 min. (d) 2.5 min. (e) 3 min

distinguished within the crystalline hard phases (See *Figure 2*).

Transmission electron microscopy. The morphology of the bulk HTPBD/2,6–TDI/BDO system was also investigated by microtoming and electron microscopy. *Figure 3* shows a spherical crystalline superstructure which was representative of the bulk sample. The sizes of these superstructures corresponded well with the sizes of the birefringent phases shown in *Figure 2*.

Solution cast films were made by dissolving the bulk sample using dimethyl formamide (DMF) as solvent. The polar nature of DMF makes it a good solvent for the hard phase, but a poor solvent for the soft hydrocarbon matrix. In *Figure 4a*, distinct boundaries between the crystalline superstructure and amorphous matrix are shown. Such large, well defined regions are indicative of the segregation of molecules of similar chemical composition and hard segment length. Moreover, there appear gel particles which are likely soft segment rich entities that are insoluble in DMF at the casting temperature of 80°C (see arrows A in *Figures 4a* and *4b*). If the solution was filtered before the film was cast the gel particles were not observed. In the solution cast films, the slow crystallization which results from the slow evaporation of the solvent promotes a better organized hard phase than in the bulk samples. The previous paper discusses the separation of these polyurethanes into fractions of different composition and their subsequent characterization[30].

HTPBD/2,4–TDI/BDO

Optical microscopy. Similar optical microscopy studies have been done on the 2,4–TDI based system. The BDO formed droplets in the PBD/2,4–TDI mixture as in the 2,6–TDI system. Most of the globular regions of BDO maintained their shape until the completion of the reaction, although coalescence of some globules occurred before the reactant mixture gelled. Because of the asymmetry of the two NCO groups on the 2,4–TDI molecule the hard segment was unable to crystallize. *Figure 5* shows a microtomed section of the bulk sample in unpolarized light. The hard phase regions can be distinguished from the soft matrix due to a difference in refractive index.

Transmission electron microscopy. *Figure 6* shows the morphology of a DMF solution cast film. Because of the polar nature of the solvent, molecules containing long hard segment sequences tend to stay in the solvent until the solution gets very concentrated, while molecules containing only short hard segment sequences and mo-

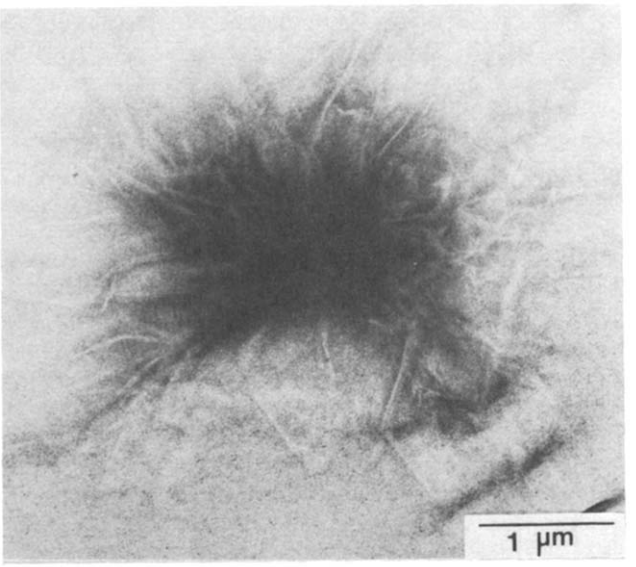

Figure 3 Electron micrograph of a cryo-microtomed thin section of HTPBD/2,6–TDI/BDO bulk sample

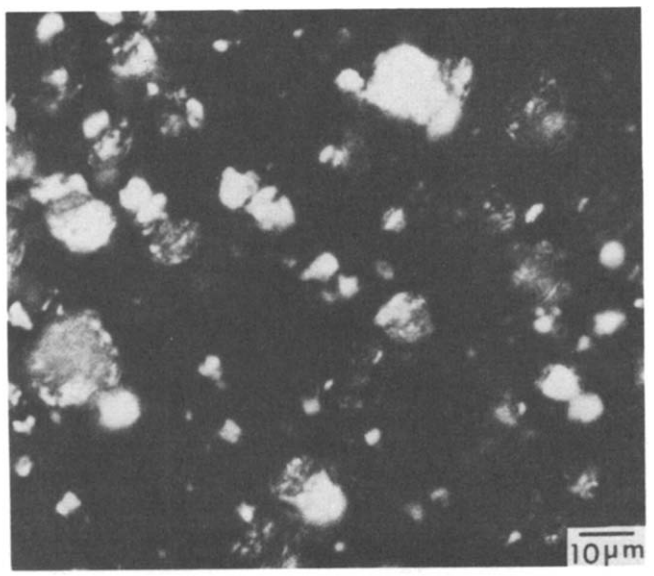

Figure 2 Optical micrograph (crossed polarizers) of a microtomed thin section of HTPBD/2,6–TDI/BDO bulk sample

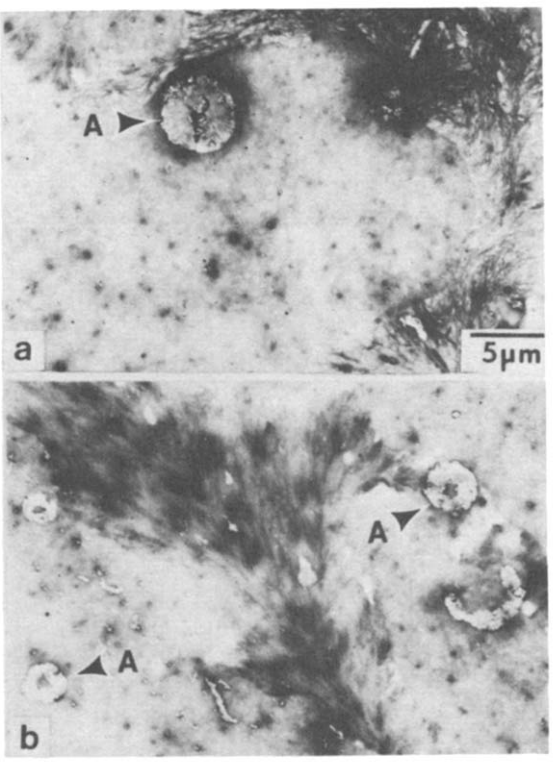

Figure 4 Electron micrograph of a DMF solution cast thin film from HTPBD/2,6–TDI/BDO bulk sample. Arrows A indicate a gel particle

lecules of pure soft segment homopolymer coagulate and precipitate out of solution earlier and segregation occurs. In *Figure 6*, discrete domains of relatively pure soft segment are clearly seen (some are indicated by arrows). Their rubbery nature is demonstrated by the way they were deformed by a crack passing through the brittle hard segment rich matrix.

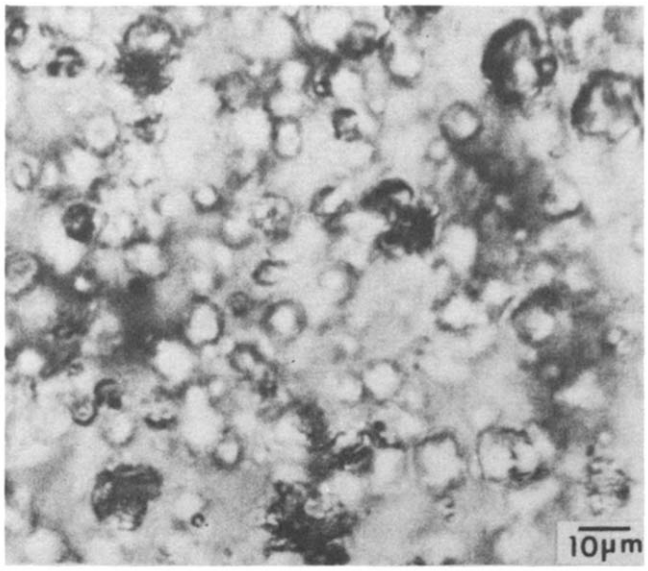

Figure 5 Optical micrograph of a microtomed thin section of HTPBD/2,4–TDI/BDO bulk sample

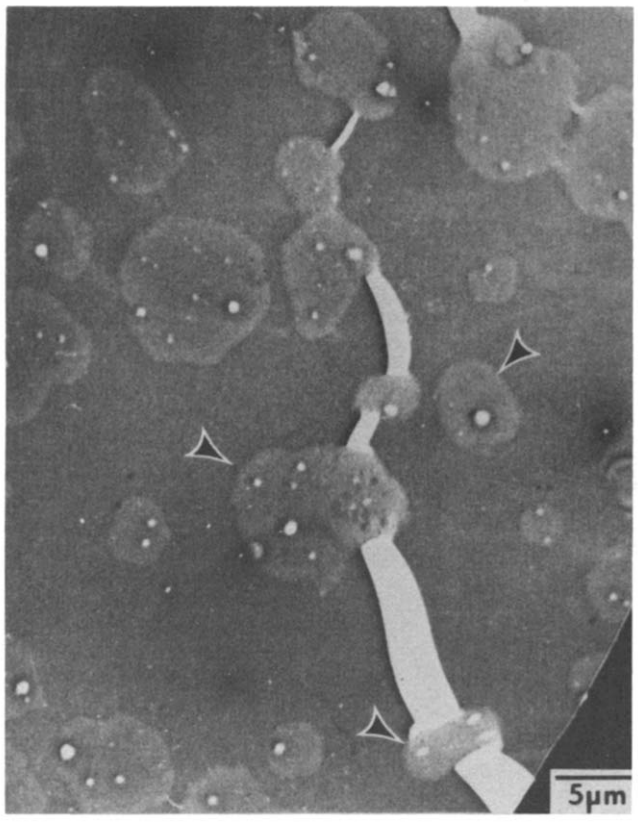

Figure 6 Electron micrograph of a DMF solution cast thin film from HTPBD/2,4–TDI/BDO bulk sample

MODEL

In *Table 1*, the relative volumes of the reactants which were used in the polymerization are listed along with the hard segment T_g's for six different compositions. Because of the low density and high molecular weight of HTPBD compared with TDI and BDO, the volume fraction of HTPBD ranges from 50% up to 86% as the hard segment content drops from 55% to 18%. Combining the morphological results with the extraction and analytic results (see Ref. 30, Table 3), three schematic models (*Figure 7a*, *7b* and *7c*) are proposed to describe the heterogeneous nature of the HTPBD/TDI/BDO system early in stage II of the reaction. *Figure 7a* describes the high hard segment content samples. In the matrix the TDI endcapped HTPBD molecules segregate to form spherical domains with their TDI endgroups outside. The free TDI molecules form a continuous phase surrounding these micro-domains. After BDO is added, the reaction between free TDI and BDO molecules within the BDO droplet will result in mostly hard segment rich molecules which contribute to the higher temperature hard segment T_g in the 2,4–TDI samples[30,31] and the high T_m observed in the 2,6–TDI sample[32]. The limited solubility of BDO molecules in the PBD/TDI matrix causes only short hard segment sequences which then give rise to the lower T_g in the 2,4–TDI samples[30,31] and lower T_m observed in the 2,6–TDI sample[32]. These types of multiple melting endotherms and glass transitions have often been seen in polyurethane systems and have been explained by segregation of hard segment sequences into groups of discrete lengths. However, no reasonable explanation has been given as to how this can take place from systems with a most probable sequence length distribution. The multiple transitions undoubtedly have to do with the approximately bimodal distribution of hard segment lengths in the matrix and the hard segment regions*.

Figure 7b describes the low hard segment content samples. At such overall compositions, PBD occupies about 80% to 90% of the volume in the PBD/TDI phase. Free TDI molecules segregate to form micro-domains, and the TDI endcapped PBD molecules form a continuous phase surrounding these domains. After BDO is added, the reaction between the free diisocyanate groups at the ends of the PBD molecules and BDO molecules

* It should be noted that multiple melting endotherms can also be caused by polymorphism which can occur in certain polyurethane systems[37].

Table 1 Summary of relative volumes of reactants used in synthesis and hard segment glass transition temperatures for samples of different compositions

Sample mole ratio HTPBD/2,4–TDI/BDO	Hard segment content % by weight	Relative volume of reactants used in synthesis			Hard segment T_g's (°C) (ref. 29)
		HTPBD	TDI	BDO	
1/10/9	55	1.0	0.63	0.33	75
1/8/7	49	1.0	0.50	0.26	74
1/6/5	42	1.0	0.38	0.18	40,65
1/4/3	32	1.0	0.25	0.11	20,55
1/3/2	25	1.0	0.19	0.07	20
1/2/1	18	1.0	0.12	0.04	20

within the droplets will result in relative short hard segment sequences in the matrix. The free TDI molecules will interdiffuse with the BDO droplets and react forming essentially regions of pure hard segment polymer.

Between high hard segment content samples and low hard segment content samples, a phase inversion must occur in the matrix phase. The highest hard segment sample investigated in this study was 55% by weight. It is conceivable that at very high hard segment concentrations there could be a phase inversion between the BDO droplets and the soft segment matrix though, this was not seen in this study. Scriven[38] has suggested that materials tend to form bicontinuous phases to minimize surface free energy at certain compositions of mixtures. Applying this idea, *Figure 7c* suggests that for the intermediate hard segment content samples, a bicontinuous structure forms. Endacpped PBD and free TDI both have opportunities to react with BDO in the BDO droplets and with BDO dissolved in the PBD/TDI phase. In this case, approximately equal populations of final polymers of long hard segment lengths and of short hard segment lengths will be found.

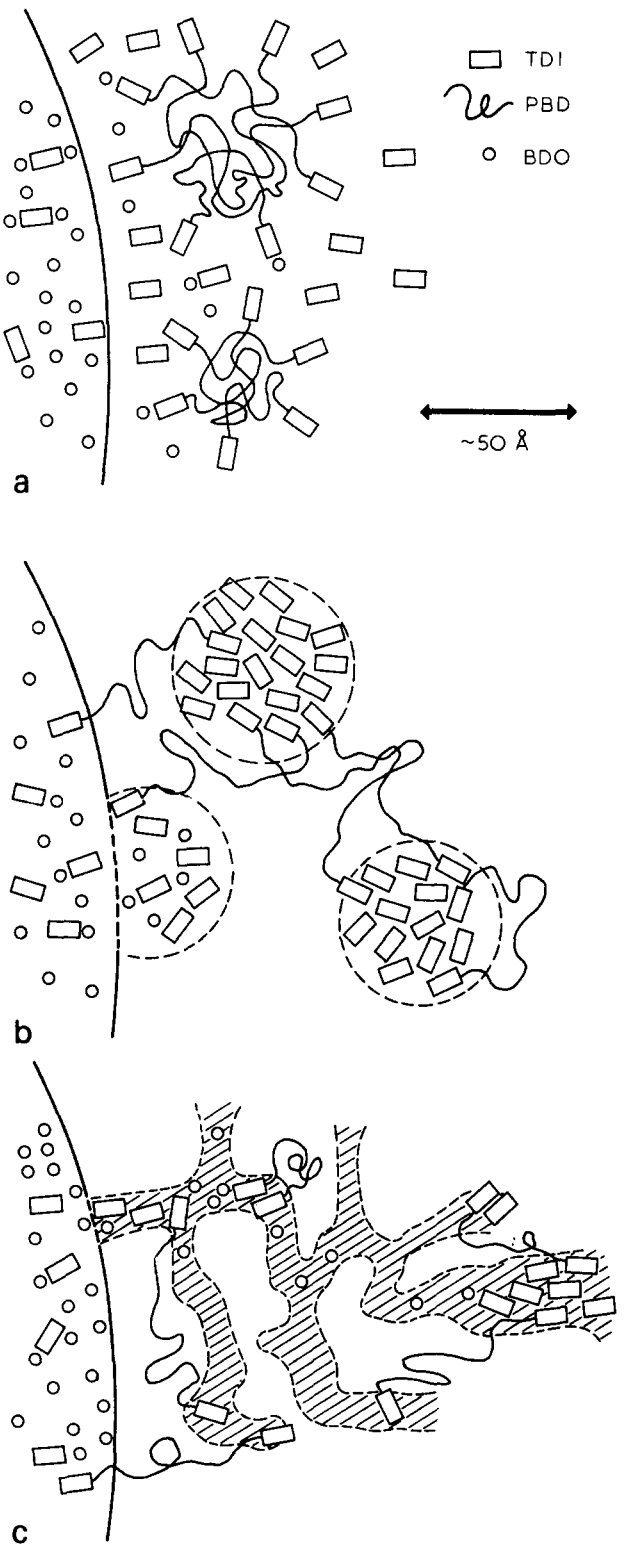

Figure 7 Schematic models depicting the microstructure during polymerization of the HTPBD/TDI/BDO polyurethane system. Left hand side of each figure shows portion of a large micron size BDO drop. (a) At high hard segment content. (b) At low hard segment content. (c) At intermediate hard segment content

PPO–EO/MDI/BDO

Optical microscopy. From preliminary compatibility tests, it was found both PPO–EO/MDI and PPO–EO/BDO were compatible on the scale of resolution of the light microscope using conventional optics. A one-stage polymerization was followed in the optical micros-

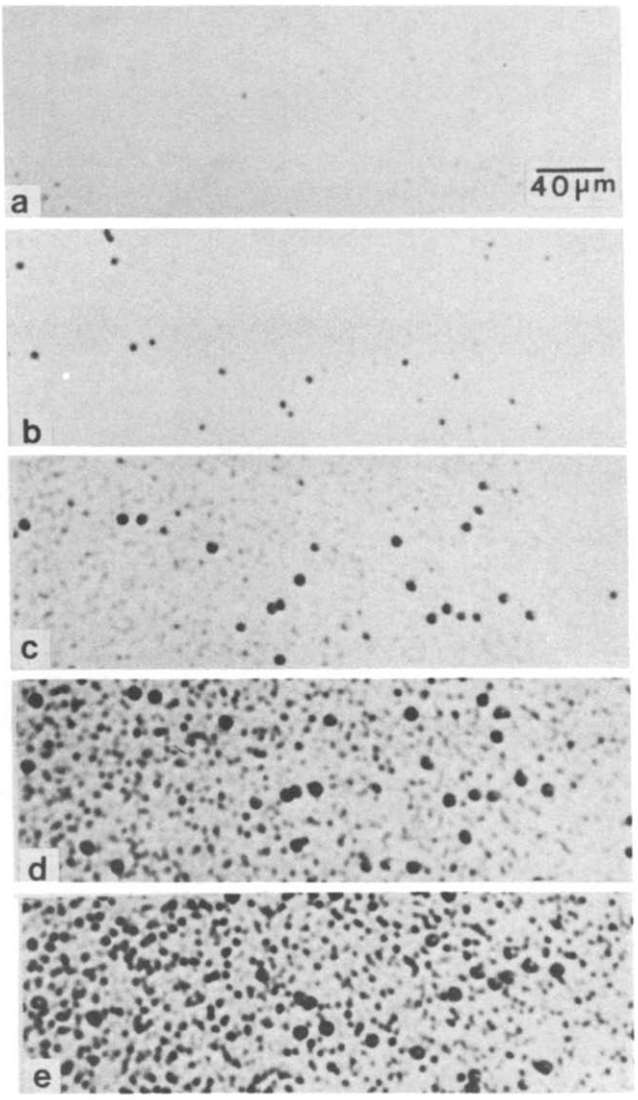

Figure 8 Optical micrographs (uncrossed polarizers) of the reacting system of PPO–EO/MDI/BDO. All micrographs are at the same magnification. (a) 100 s after the mixing of the three components. (b) 110 s. (c) 120 s. (d) 130 s. (e) 180 s

cope (see *Figures 8a–8e*). Upon first mixing of the three components, the reacting fluid appeared transparent and homogeneous. After rapidly stirring for 30 s one drop of the still transparent reactant solution was pressed into a thin film between two glass slides and transferred to the hot stage. After 100 s from the start of the mixing, a few small dark spherical structures began to appear in the background. As the reaction proceeded, these structures grew in size. Approximately three minutes after the first mixing, the system became stationary. The spherical structures that appeared first in the reaction were identified as hard segment rich spherulites as can be seen in *Figures 9a* and *9b*. After about 120 s (*Figure 8c*) a second type of structure began to appear from the background. This structure was apparently nucleated at a later time than the spherulites. This second structure continued to grow but never became as large as the spherulites, nor did it develop any visible birefringence. These second structures were probably the globules which were seen in the bulk morphology studies discussed earlier[34–36] (ref. 36 Figure 25d). The spherulites that appeared early in the reaction could be due to heterogeneous nucleation on dust particles. These heterogeneous nuclei could cause faster phase growth and promote crystallization. The globules which appeared slightly later in the reaction never do crystallize, possible due to the absence of suitable nuclei. These globules may be transformed, as shown by the study of Chang *et al.*[34], after annealing at high temperature due to the molecules migrating and crystallizing with the neighbouring spherulites.

It is interesting to speculate about the origins of the spherical structures which are formed from the homogeneous reactant mixture. It can be postulated that reactant phase separation occurs below the micron scale which does not show up at first in the optical microscope, but due to diffusion and reaction of other molecules into these micro-phases, the size and the composition of these structures change. When they grow large enough, they become detectable. Although the incompatibility between polypropylene oxide (PPO) and BDO is reduced by endcapping PPO with polyethylene oxide, and the mixture of the two appears homogeneous to the unaided eye, the molecular segregation of BDO molecules or segment segregation of PPO–EO may still occur in the sub-micron level depending on the volume fraction of each reactant. On the other hand, MDI molecules may also segregate due to the molecular level incompatibility with the PPO segments. The models suggested for the PBD/TDI phase (*Figure 7*) may still be applied to this more complicated system.

Alternatively, the reacting mixture could be completely homogeneous with precipitation and crystallization occurring as the molecular weight of the reacting species increases and the presence of suitable nuclei is what controls the ratio of globules to spherulites. To answer these questions more work is needed to elucidate the morphology at the submicron scale during the reaction in the PPO–EO/MDI/BDO system.

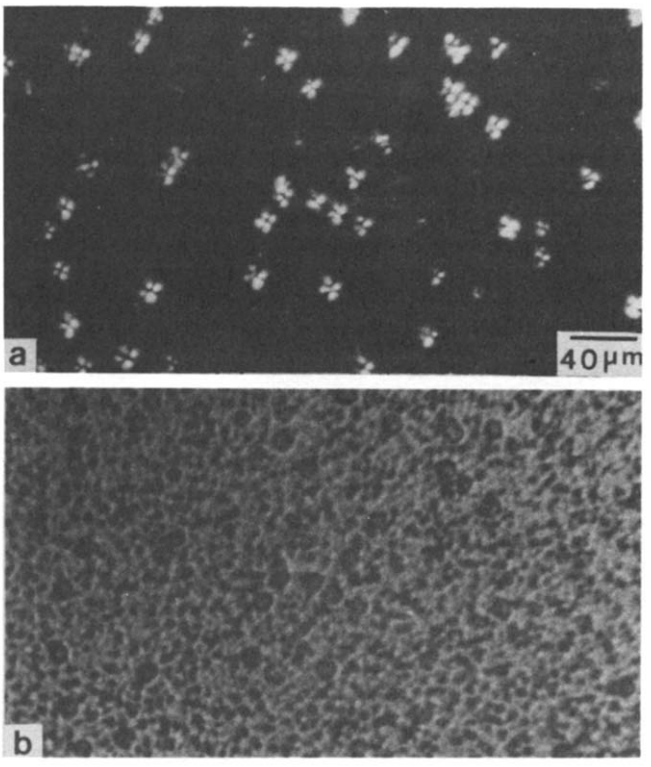

Figure 9 Optical micrographs of PPO–EO/MDI/BDO sample 13 min after the mixing of the three components. (a) Crossed polarizers. (b) Uncrossed polarizers

CONCLUSIONS

(1) The incompatible nature of HTPBD and BDO is found to greatly influence the morphology of HTPBD/TDI/BDO polyurethanes. Micron size phases exist throughout the reaction. The resulting polymer is a mixture of copolymers having a bimodal distribution of hard segment lengths.

(2) The common finding in several segmented polyurethanes was that the system has two hard-segment glass-transition temperatures and/or multiple melting endotherms. These features are a consequence of the incompatibility of the reactants.

(3) Models of phase separation which are suggested in this paper can explain the formation of a bimodal distribution of hard segment lengths in the polymerized samples.

(4) The PPO–EO/MDI/BDO system exhibit no visible macroscopic reactant separation initially, but microphase separation of reactants and products probably occurs below the micron scale during the initial part of the polymerization and leads to micron scale heterogeneties.

ACKNOWLEDGEMENTS

Acknowledgement is made to the Army Research Office, Durham, under grant no. DAAG 2980C0054, the National Science Foundation, grant CPE-8118232, Chemical and Process Engineering (Industrial-Academic Program), and to Union Carbide, Chemical and Plastics, South Charlestown, West Virginia, for financial support. The authors are also pleased to acknowledge helpful discussions with Professor C. W. Macosko of the University of Minnesota and Professor J. M. Ottino of the University of Massachusetts and the technical assistance of Mr D.-J. Lin.

REFERENCES

1 Cooper, S. L. and Tobolsky, A. V. *J. Appl. Polym. Sci.* 1966, **10**, 1837
2 Bonart, R. *J. Macromol. Sci.-Phys.* 1968, **B2(1)**, 115
3 Clough, S. B., Schneider, N. S. and King, A. O. *J. Macromol. Sci.-Phys.* 1968, **2**, 64

4 Seymour, R. W., Estes, G. M. and Cooper, S. L. *Macromolecules* 1970, **3**, 579
5 Huh, D. S. and Cooper, S. L. *Polym. Eng. Sci.* 1971, **11**, 369
6 Critchfield, F. E., Koleske, J. V., Magnus, G. and Dodd, J. L. *J. Elastoplastics* 1972, **4**, 22
7 Allport, D. C. and Mohajer, A. A. *Block Copolymers* (Eds. D. C. Allport and W. H. James), Appl. Sci. Publ. 1973, 443
8 Seymour, R. W. and Cooper, S. L. *Macromolecules* 1973, **6**, 48
9 Seefried, C. G., Koleske, J. V., Critchfield, F. E. and Dodd, J. L. *Polym. Eng. Sci.* 1975, **15**, 646
10 Seefried, C. G., Koleske, J. V. and Critchfield, F. E. *Polym. Eng. Sci.* 1976, **16**, 771
11 Manson, J. A. and Sperling, L. H. 'Polymer Blends and Composites', Plenum Press 1977, 153
12 Noshay, A. and McGrath, J. E. 'Block Copolymers', Academic Press 1970, 370
13 Ferguson, J. and Ahmad, N. *Eur. Polym. J.* 1977, **13**, 865
14 Lagasse, R. R. *J. Appl. Polym. Sci.* 1977, **21**, 2489
15 Lunardon, G., Sumida, Y. and Vogl, O. *Makromol. Chem.* 1980, **87**, 1
16 Bonart, R., Morbitzer, L. and Hentze, G. *J. Macromol. Sci.-Phys.* 1969, **B3(2)**, 334
17 Koutsky, J. A., Hein, J. V. and Cooper, S. L. *J. Polym. Sci. Polym. Lett. Edn.* 1970, **8**, 353
18 Bonart, R., Morbitzer, L. and Muller, E. H. *J. Macromol. Sci.-Phys.* 1974, **B9(3)**, 447
19 Schneider, N. S., Desper, Illinger, J. L., King, A. O. and Barr, D. *J. Macromol. Sci.* 1975, **B11**, 527
20 Chang, A. L. and Thomas, E. L. **ACS Adv. Chem.** 1979, **176**, 31
21 Peebles, Jr., L. H. *Macromolecules* 1974, **7**, 6
22 Peebles, Jr., L. H. *Macromolecules* 1976, **9**, 1, 58
23 Castro, J. M., López-Serrano, F., Camargo, R. E., Macosko, C. W. and Tirrell, M. *J. Appl. Polym. Sci.* 1980, **26**, 2067
24 Hagar, S. L., Mackury, T. B., Gerkin, R. M. and Critchfield, F. E. *ACS Symp. Ser.* 1981, 172
25 Camargo, R. E. *PhD Thesis*, University of Minnesota, 1983
26 Nesterov, A. E., Lipatova, T. E., Dusek, K., Pelzbauer, Z., Honska, M., Hradil, J. and Lipatov, Y. S. *Makromol. Chem.* 1976, **52**, 39
27 Tirrell, M., Lee, L. J. and Macosko, C. W. 'Polymerization Reactors and Processes', ACS Press 1979, Washington, DC
28 Xu, M., Hu, S., Wu, M., Chen, C. and Jin, Y. *Polym. Commun.* 1982, **1**, 27
29 Foks, J. and Janik, H. Proceedings of European Plastics Conference, Paris, June, 1982
30 Xu, M., MacKnight, W. J., Chen, C. H. Y. and Thomas, E. L. *Polymer* 1983, **24**, 1327
31 Brunette, C. M., Hsu, S. L., MacKnight, W. J. and Schneider, N. S. *Polym. Eng. Sci.* 1981, **21**, 668
32 Brunette, C. M. and MacKnight, W. J. *Rubber Chem. Tech.*, in press
33 Zdrahala, R. J., Gerkin, R. M., Hager, S. J. and Critchfield, F. E. *J. Appl. Polym. Sci.* 1979, **24**, 2041
34 Chang, A. L., Briber, R. M., Thomas, E. L., Zdrahala, R. J. and Critchfield, F. E. *Polymer* 1982, **23**, 1060
35 Fridman, I. D., Thomas, E. L., Lee, L. J. and Macosko, C. W. *Polymer* 1980, **21**, 393
36 Schmitt, B. J. *Angew. Chem. Int. Ed. Engl.* 1979, **18**, 273
37 Briber, R. M. Proceedings of the Electron Microscopy Society of America, Annual Meeting 1982, 674
38 Scriven, L. E. *Nature* 1976, **263**, 123